Article II

Laponite Functionalized with Biuret and Melamine – Application to Adsorption of Antibiotic Trimethoprim.

Microporous and Mesoporous Materials 253 (2017) 112–122

Contents lists available at ScienceDirect

Microporous and Mesoporous Materials

journal homepage: www.elsevier.com/locate/micromeso

Laponite functionalized with biuret and melamine – Application to adsorption of antibiotic trimethoprim

Beatriz González [a], Tiago H. da Silva [b], Katia J. Ciuffi [b], Miguel A. Vicente [a, *], Raquel Trujillano [a], Vicente Rives [a], Emerson H. de Faria [b, **], Sophia A. Korili [c], Antonio Gil [c]

[a] GIR-QUESCAT, Departamento de Química Inorgánica, Universidad de Salamanca, 37008 Salamanca, Spain
[b] Universidade de Franca, Av. Dr. Armando Salles Oliveira, Parque Universitário, 201, 14404-600, Franca, SP, Brazil
[c] Departamento de Química Aplicada, Edificio de los Acebos, Universidad Pública de Navarra, Campus Arrosadía, 31006 Pamplona, Spain

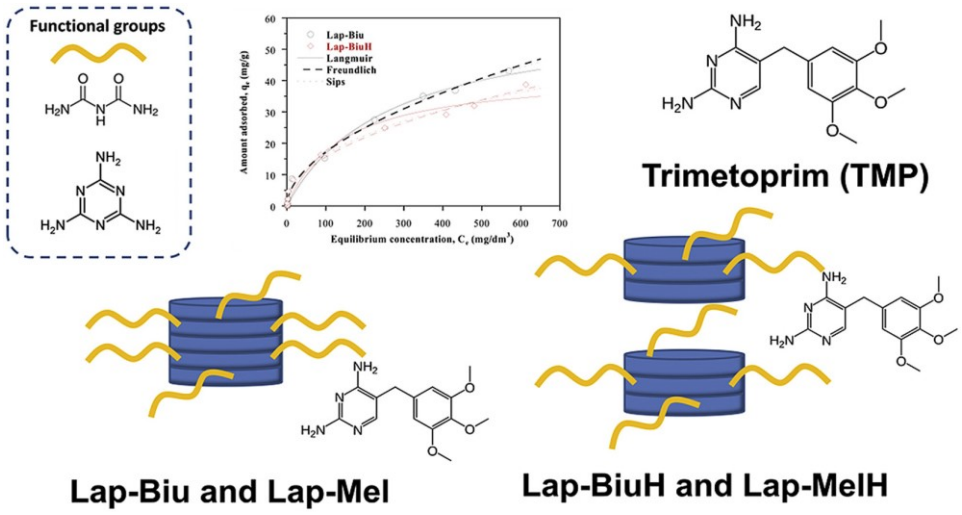

ABSTRACT

Laponite-aminosilane hybrid materials have been prepared by reaction of a chlorosilane, (3-chloropropyl)triethoxysilane, with two aminated compounds, namely, biuret or melamine. The resulting compounds were used for the functionalisation of laponite, using two synthesis procedures. The hybrid materials thus formed were fully characterised, and tested for the adsorption of the antibiotic Trimethoprim (trimethoxybenzyl-2,4-pyrimidinediamine). The characterisation results showed that functionalisation was successful, and the adsorption experiments showed a high affinity of the hybrid materials for the removal of Trimethoprim, with removal percentages larger than 80%.

Keywords: Laponite; Biuret; Melamine; Organophilization; Clay; Trimethoprim adsorption.

1. Introduction

Clay minerals are hydrophilic materials, but for several uses it is even mandatory, to confer their surface an organophilic nature by the incorporation of organic species to favour their interaction with other organic species (polymers, pollutants, etc.) (Christidis, 2013; de Paiva et al., 2008). Among such uses, the formulation of Clay-Polymer Nanocomposites (CNP) is particularly important, but the use of clay minerals in the preparation of paints, cosmetics or personal care products, in the adsorption of pollutants, or as rheological control agents, are other relevant applications that require the clay minerals having an organophilic surface. The organic species incorporated may act as ligands to metal cations, allowing the preparation of catalysts, sensors, luminescent agents, etc. For these reasons, organophilisation of clay minerals has been widely studied.

The strategy for organophilisation is usually fitted to the clay minerals considered. For instance, tetrasubstituted quaternary alkyl-ammonium ions have been mainly used to functionalise swellable smectites, by intercalation in the interlayer region with substitution of their natural occurring charge-balancing exchangeable cations; these preparations are even commercially available (Cloisite®). Grafting of organo-silanes on several clays, particularly silanes containing other functional groups such as amine, mercapto or chlorine, has received increasing interest in the last years, opening new potential applications for these materials (Detellier and Letaief, 2013; Lagaly and Dékány, 2013).

Kaolinite can be organophilised by a multi-step, host-guest displacement method, beginning with small and very polar molecules, and then substituting them by the final functionalising molecules. This special procedure is used because kaolinite has no exchangeable cations and the organophilising species cannot be intercalated by ionic exchange, and swelling of the strongly bonded layers being very difficult (Lagaly et al., 2013).

Laponite is a commercially available synthetic hectorite. It exfoliates very easily in aqueous dispersion, and solid samples do not show a long order in their stacking direction. Its exchangeable cations can be substituted by cationic species, but without intercalation. Functionalisation of laponite has been scarcely studied (Borsacchi et al., 2007) and grafting on the external surface of its layers seems to be the optimal procedure.

Biuret (2-imidodicarbonic diamide), also known as carbamylurea (see its formula in Fig. II.1) results from the condensation of two urea molecules removing one ammonia

molecule. It is the reference for the Biuret reaction, widely used for the identification of proteins and peptides, as peptide bonds react as the biuret molecule does. Biuret is also used to denote the functional group -(HN-CO-)$_2$N-, and can be viewed as the result of the trimerization of isocyanates. Biuret has been used as an alternative to urea as a non-protein nitrogen source for animal feed. Melamine (1,3,5-triazine-2,4,6-triamine, Fig. II.1) can be formally be considered as a trimer of cyanamide; it has fire-retardant properties, and it is widely used to form, by combination with formaldehyde, the resin also known as melamine, used in decorative laminates, insulation (melamine foam) and cement admixture (sulfonated melamine formaldehyde).

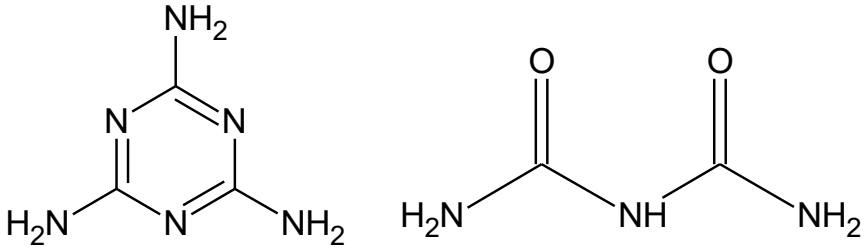

Fig. II.1. Chemical structures for melamine (left) and biuret (right).

In recent years, pharmaceutical products and their derivatives have become of great environmental concern. These compounds may be released to the environment in different ways: disposing of component precursors, disposal of by-products of the manufacturing process, and consumption/elimination of drugs (Bekçi et al., 2007; Molu and Yurdakoç, 2010; Richardson et al., 2005). One of the largest concerns related to this fact is the development of resistant organisms, mainly to antibiotics. Trimethoprim [5-(3,4,5-trimethoxybenzyl) pyrimidine-2,4-diamine] (TMP) is an antibacterial drug used to treat infections, and may inhibit a variety of gram-positive and gram-negative bacteria (Liu et al., 2017), and so being currently used as an antibacterial agent. However, TMP is incompletely metabolised by the human being during the therapeutic process, and about 80% is excreted in its pharmacologically active form (Ji et al., 2016; Liu et al., 2017; Zhang et al., 2016).

Both biuret and melamine contain three amine groups, able to condense with other groups, the three groups being able to condense under appropriate conditions. The chlorosilane (3-chloropropyl)triethoxysilane (abbreviated ClPTES) was chosen for such a condensation reaction. The resulting compounds were used for functionalisation of Laponite, and the functionalised solids, after their complete characterisation, were studied for their ability to adsorb Trimethoprim.

2. Experimental

2.1 Preparation of the hybrid materials

2.1.a. Non-aqueous route. The first step was the condensation between the chlorosilane and the amino derivatives, Fig. II.2. A given mass of the amino precursor (4.31 g, 0.041 mol) of biuret (Biu) or 5.23 g (0.041 mol) of melamine (Mel) was reacted with 10.5 mL (0.041 mol) of (3-chloropropyl)triethoxysilane (ClPTES) using toluene as solvent. The mixture was magnetically stirred in glass flasks for 4 h, under an anhydrous nitrogen atmosphere, at 80 ºC, using a conventional reflux setup. The condensation reaction is schematized in Fig. II.2; one, two or even all three amine groups in each amine molecule can condensate with the silane. *A priori*, it is expected that only one amine group condenses, as the ClPTES:organic compound (Mel or Biu) molar ratio was fixed to 1:1. However, the amine groups could condense also with the silanol groups from the clay, and also the hydroxyl groups from the silane, and so the final condensation degree can change. After 4 hours of reaction, 10.0 g of Laponite were added to each solution and the suspension was maintained under vigorous stirring for 24 h. The resulting materials were washed 3 times with toluene and 5 times with ethanol and oven-dried at 80 ºC; the resulting solids are designated as "Lap-Biu" and "Lap-Mel", respectively.

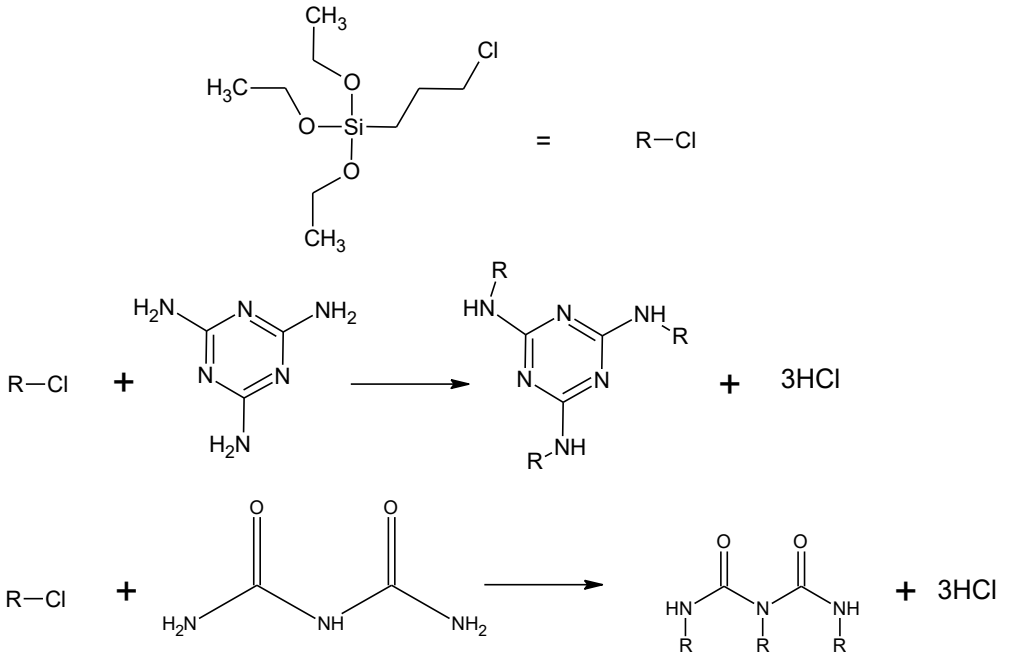

Fig. II.2. Complete condensation reactions between ClPTES and biuret or melamine for the synthesis of new aminosilanes.

2.1.b. Aqueous route. An amount of 10.0 g of Laponite was suspended in 200 mL of water under vigorous stirring to obtain a swollen Laponite gel. Then 10.5 mL (0.041 mol) of ClPTES were slowly added to the suspension and the resulting mixture was vigorous stirred for 1 h at room temperature and then 4.31 g (0.041 mol) of Biu or 5.23 g (0.041 mol) of Mel were added, and the system was maintained under stirring for 24 h at room temperature (ca. 25 ºC). Two drops of HCl were used to initiate the hydrolysis, and more HCl is generated during the process (Fig. II.2). The ClPTES:organic compound (Mel or Biu) molar ratio was fixed to 1:1. The resulting materials were washed and dried as described for the previous method, and they were named as "Lap-BiuH" and "Lap-MelH", respectively.

2.2. Characterisation techniques

Element chemical analyses were carried out at Activation Laboratories Ltd., in Ancaster, Ontario, Canada, using inductively coupled plasma (ICP) for the metallic elements, IR spectroscopy after combustion for C and Kjeldahl method for N determination.

The powder X-ray diffraction (PXRD) diagrams of the solids were recorded in a Siemens D-500 diffractometer operating at 40 kV and 30 mA, using filtered Cu Kα radiation in the 2º to 65º (2θ) range. All the analyses were carried out at a scan speed of 2º/min.

The thermal analyses were carried out in a TA Instruments SDT Q600 simultaneous DTA-TGA thermal analyzer, at temperatures ranging from 25 to 900ºC, at a heating rate of 10ºC/min and under air flow (100 mL/min).

The infrared absorption spectra were recorded in a Perkin-Elmer Spectrum One FTIR spectrometer, using the KBr pellet technique.

The BET specific surface area and porosity data of the solids were calculated from their nitrogen adsorption-desorption isotherms at –196 ºC, carried out in a Micromeritics Gemini VII 2390T apparatus. The samples were previously treated at 110°C under a stream of N_2 for 2 h, in a Micromeritics Flowprep 060 equipment.

Scanning electron microscopy (SEM) was performed using a Carl Zeiss SEM EVO HD25 apparatus with a thermionic LaB_6 filament cannon as the electron source. The samples were coated with a thin gold layer by evaporation using a Bio-Rad ES100 SEN coating system.

2.3. Adsorption of Trimethoprim using the batch method

The adsorption experiments were carried out using the batch method. For all the experiments, the concentration of TMP in the solutions was determined by UV/Visible spectroscopy, using a Hewlett-Packard 8453 Diode Array spectrometer. The absorption was measured at 288 nm, the wavelength corresponding to the maximum absorbance of the molecule under the conditions used. The absorbance at this wavelength showed a linear response, according to the Beer-Lambert law, in the concentration range from 1 to 50 mg/L, which was used in the experiments.

2.3.a. Trimethoprim adsorption kinetics. The kinetics experiments of TMP adsorption onto the adsorbents (Lap-Biu, Lap-Mel, Lap-BiuH and Lap-MelH), were carried out in glass vials by shaking at room temperature a known amount of an adsorbent, typically 50 mg, and 5.0 mL of an aqueous TMP solution with a concentration of 50 mg/L. At pre-determined time intervals between 1 and 150 min, the TMP concentration in the supernatant was analyzed, to calculate the amount of TMP adsorbed onto the solid, according to Equation 1:

$$q_t = \frac{V \cdot (C_i - C_t)}{m} \qquad \text{Equation 1}$$

where q_t (mg/g) is the amount of TMP adsorbed at time t (min), C_i (mg/L) is the initial TMP concentration in the solution, C_t (mg/L) is the TMP concentration in the solution at time t, V (L) is the volume of the solution, and m (g) is the mass of adsorbent used.

Unfortunately, it was not possible to perform the adsorption experiments with the original Laponite, as, when it is immersed in water, a gelation process occurs, making it extremely difficult to separate the liquid from the solid. Thus, it was not possible to compare the results of the hybrid materials with the starting, unloaded Laponite.

2.3.b. Trimethoprim adsorption equilibrium. The equilibrium experiments at 25 °C were carried out in glass vials by shaking for 20 min a known amount of the adsorbent, typically 50 mg, with 5.0 mL of TMP solution at the desired TMP concentration, typically ranging from 1 to 1000 mg/L. Then, the clay was separated from the supernatant by centrifugation at 3500 rpm for 15 min. The concentration of TMP remaining in the

supernatant was determined, and the amount of adsorbed dye was calculated using Equation 2:

$$q_e = \frac{V \cdot (C_i - C_e)}{m} \qquad \text{Equation 2}$$

where q_e (mg/g) is the amount of adsorbed TMP; C_i and C_e (mg/L) are the initial and equilibrium liquid-phase concentrations of the organic compound, respectively; V (L) is the volume of the solution; and m (g) is the amount of adsorbent.

3. Results and discussion

3.1 Characterisation of the adsorbents

The PXRD diagrams of the solids are shown in Fig. II.3. As expected, the diagram for parent Laponite does not show a long order in its basal reflection, but only a shoulder close to 6º (≈ 15 Å). The intralayer reflections, independent of layer stacking, mainly (02,11), ($\bar{2}02$) and (06,33), are, however, clearly evidenced. Incorporation of the aminosilanes leads to noticeable changes in the diffractograms. The changes observed differ depending on the preparation method. In the case of the non-aqueous route, the clay layers are markedly ordered, and the basal reflection is observed as a low intense peak when biuret is used, and as a clear peak, with a basal spacing of 12.5 Å, in the case of melamine. This suggests that grafting of the silane molecules on Laponite induces the layers to orientate parallel between them, thus originating the enhancing of the (001) reflection. The number of stacked layers seems to be larger in the case of melamine, as concluded from the somewhat narrower peak recorded, probably because the melamine molecule is flat itself, and the derived silane may maintain a mostly flat disposition.

When the samples are prepared under aqueous conditions, the stacking is even lower than in original Laponite: the solid obtained using biuret (Lap-BiuH) is completely delaminated, while that one obtained with melamine shows only a residual shoulder due to the basal reflection. So, formation of the aminosilane previously to its interaction with the clay clearly favors ordering of the layers in the resulting solids. Concerning the intralayer reflections, they are weaker in all the treated solids than in parent Laponite, suggesting a certain degradation of the layers, although *a priori* the layers should not be affected by the reaction conditions.

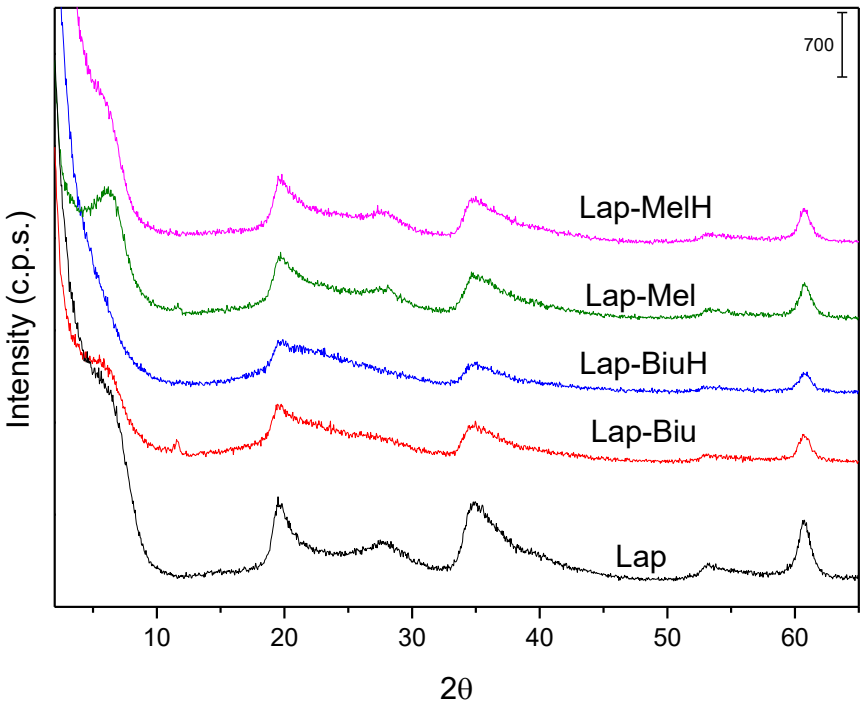

Fig. II.3. PXRD patterns of original Laponite and of the derived solids.

Some differences in the chemical compositions are observed among the grafted materials, and also when they are compared to parent Laponite (Table II.1). As usual for this sort of solids, the chemical composition is given in terms of the oxides of the existing elements and, for the functionalised samples, the content of carbon and nitrogen has been also determined. The solids have different contents of water and organic matter, and consequently the sum of the contents of the metal oxides (in other words, of raw Laponite) was different for each solid. Comparison among the compositions of the solids is difficult; it is observed that fixation of the organic matter produces a significant decrease in the content of MgO, Na_2O and CaO, while no change is observed for Fe_2O_3 and almost constant values were measured for Al_2O_3. The SiO_2 content is similar in all solids, as the relative decrease originated by the fixation of organic matter is somewhat balanced by the increase of silicon content upon fixation of the silane. The content on dry basis, normalising to a value of 100% the sum of the metal oxides content and elemental C and N, is given in Table II.S1 (Supplementary Information), but it is not possible to normalize the composition referred to an "internal standard". The SiO_2 content is usually used as internal standard to analyze the changes in the chemical composition of treated clays, as the tetrahedral layer containing the Si cations is hardly affected by the treatments; however, this is not possible in the current case, because of

the cited increase in silicon content upon incorporation of the silane. The other main component of Laponite, MgO, is very sensitive to acidic conditions, and the results reported in Table II.1 indicate that Mg^{2+} cations from the octahedral layers have undergone lixiviation, so it is not suitable either to be used as an internal reference.

Table II.1

Chemical composition (%w/w) of the samples

Sample	SiO_2	MgO	Al_2O_3	Fe_2O_3	Na_2O	CaO	C	N	Total
Lap	53.90	23.85	0.05	0.03	2.56	0.17	–	–	80.56
Lap-Biu	54.44	14.94	0.06	0.03	0.12	0.12	5.52	0.5	75.73
Lap-BiuH	58.48	12.36	0.06	0.03	0.02	0.02	8.99	0.3	80.26
Lap-Mel	54.43	18.33	0.04	0.03	0.03	0.05	7.10	1.8	81.81
Lap-MelH	52.30	17.62	0.06	0.03	0.02	0.01	5.65	2.7	78.39

Although the results cannot be compared on a reference basis, some effects are remarkable. First of all, the chemical composition of raw Laponite is compatible with literature data (Bandeira et al., 2012; Iurascu et al., 2009). The amount of organic matter fixed (on the basis of elemental C and N) is high, 8-11% in the dry solids, although it is even higher, on considering hydrogen and oxygen from the organic moieties (the hydrogen and oxygen contents have not been determined, as they exist in the solids under different forms, in the layers, as water, in the organic components, hydroxyl groups, etc.). Na^+ and Ca^{2+} cations are almost completely removed, which suggests that the incorporation of the organic matter occurs by a cation exchange reaction. The decrease in the MgO content is very marked, even higher than the relative decrease due to the incorporation of SiO_2 and organic matter, which indicates that part of octahedral Mg^{2+} is actually dissolved in the conditions used to prepare the samples. As commented above, the amount of SiO_2 seems to remain almost constant, but this indicates a significant relative increase that compensates the relative decrease caused by the incorporation of organic matter.

The absence of an internal reference makes not possible to correlate the amounts of SiO_2 (as silane) and of organic matter incorporated during the functionalisation process. However, the amounts of C and N allow to discuss on the degree of condensation between the silane and the aminated molecules, as the molar ratio between these two elements is different depending on the condensation of one, two or the three amine groups of each molecule (see

SI). As indicated, the functionalisation occurs by cation exchange (almost complete removal of sodium and calcium), so the amine groups may be protonated by the HCl molecules generated (Fig. II.2) during the condensation reactions. In addition, in the samples prepared via the aqueus route, the –OEt groups may be hydrolyzed by water. Thus, different final functionalising species are possible.

The C/N mass ratio was 11.0, 29.9, 3.95 and 2.1 for Lap-Biu, Lap-BiuH, Lap-Mel and Lap-MelH solids, respectively. Except for Lap-BiuH, for which the chemical analysis provides a low N content, these results are compatible with the condensation of all the amine groups in the molecules. For instance, in the case of Lap-Mel solid, the experimental C/N mass ratio is 3.95, while the theoretical values are 1.7, 3.0 and 4.3 if one, two or all three amine groups condense (reactions shown in Scheme I, Supplementary Information). It may be even considered that if HCl molecules generated during the condensation produce the hydrolysis of the ethoxide groups, the C/N ratio should slightly decrease, as two C atoms should be removed from the condensated molecule for each hydrolysis step.

So, the functionalisation mainly occurs by cation exchange. The difference between both methods may mainly be the hydrolysis of the ethoxide groups, that may be fast in the aqueous route by the presence of water, and much slower and in a lower extent in the non-hydrolytic method due to the HCl molecules generated by the condensation reaction (Scheme I). The acidic conditions may simultaneously favour the protonation of the amine groups, resulting in protonated species able to exchange the charge balancing cations of the clay.

The FTIR spectra of the solids are included in Fig. II.4. The incorporation of the organic components was clearly concluded from the changes in the spectra, upon comparison with that of parent Laponite. The spectrum for Laponite showed the characteristic stretching bands at 3690 cm^{-1} (MgO-H), 655 cm^{-1} (Mg-O) and 1010 cm^{-1} (Si-O) (Bandeira et al., 2012; Pereira et al., 2008), together with the bands corresponding to stretching and bending modes of water molecules. In the samples functionalised with ClPTES/Biu, intense bands attributed to biuret were observed at 1700, 1630, 1500 and 1340 cm^{-1}, due to vibrations of the C=O, N-H, C-N and C-N-C groups, respectively (Hua-Feng, 2017). In addition, changes were observed in the Si-O region, with bands close to 1000 and 1100 cm^{-1}, attributed to the Si-O vibrations from the clay and new bands from the Si-O bonds derived from the silane. For the melamine-based materials, bands corresponding to the organic molecule were also recorded at 2929, 1545, 1377 and 780 cm^{-1}, attributed to CH groups from the silane, the C=N group of the

central ring of melamine and NH groups from primary or secondary amines (Lagaly and Dékány, 2013; Stolz et al., 2016).

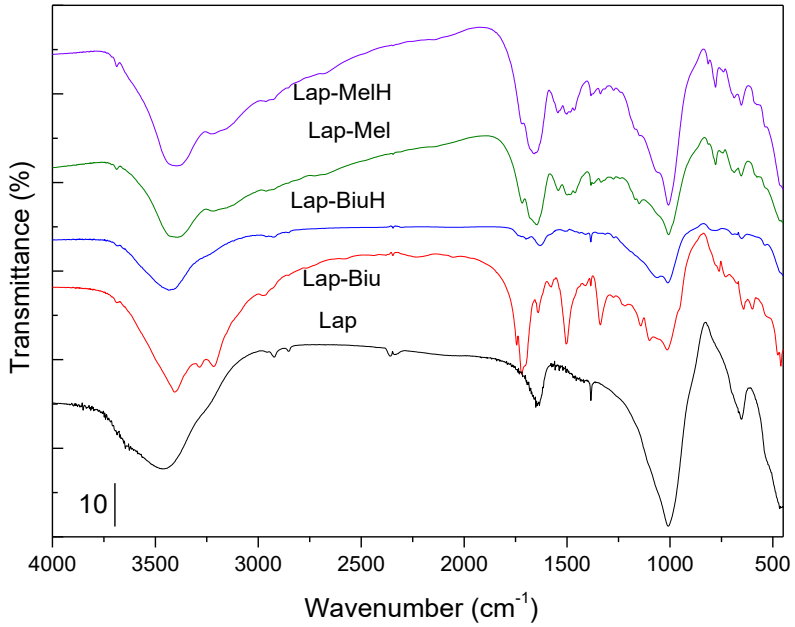

Fig. II.4. FT-IR spectra of both series of solids.

The nitrogen adsorption-desorption isotherms on the solids are shown in Fig. II.5. The isotherms can be classified as Type IV, with a H2 type hysteresis loop, in the case of Lap, Lap-BiuH and Lap-MelH, and as Type IIb, with hysteresis-loop H3, for samples Lap-Biu and Lap-Mel (Pálková et al., 2010; Zid et al., 2017; Zimowska et al., 2016, 2013). The textural properties of the solids are summarized in Table II.2. The BET specific surface area and the pore volume values of Laponite are similar to those reported in the literature (Iurascu et al., 2009; Zid et al., 2017). The synthetic route had a great influence on the evolution of the textural properties, and so the aqueous route promoted a strong increase in the specific surface area and in the pore volume, while the non-hydrolytic route led to a decrease of these values, specially for sample LapMel. This difference may be related to the structural changes undergone by the materials, as concluded from the X-ray diffraction diagrams (Fig. II.3): while the aqueous route led to highly delaminated solids, the non-aqueous route induced a stacking of the layers, where the organic molecules may occupy a large extent or almost the totality of the interlayer space; even it is possible that the organic molecules are simply blocking the access to the interlayer space.

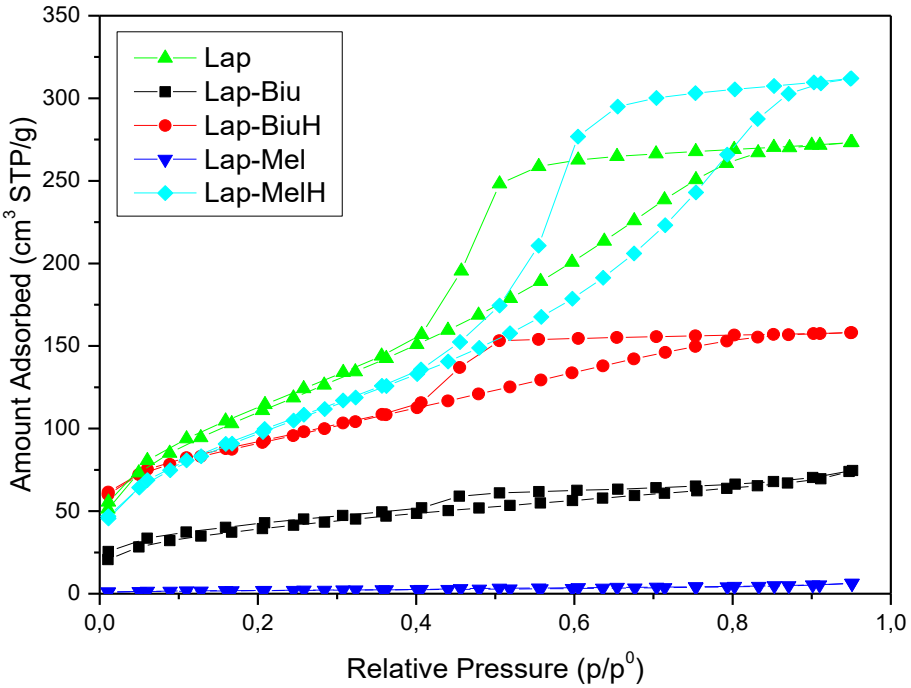

Fig. II.5. Nitrogen adsorption-desorption isotherms at –196 ºC for the solids.

Table II.2

Specific surface area and pore volume of Laponite and its derivatives.

	S_{BET} (m^2/g)	V_p (cm^3/g)
Lap	307	0.245
Lap-Biu	135	0.115
Lap-BiuH	407	0.423
Lap-Mel	7	0.010
Lap-MelH	360	0.482

The aqueous route under acidic conditions promotes the increasing of the basal space of Laponite, suggesting the intercalation of the organomodified alkoxide. As a result, the presence of siloxane and silanol groups and of Mg-OH groups on the interlaminar surface promotes the increase in the specific surface area of the materials prepared by the aqueous route (Table II.2); however, the use of a non polar solvents (toluene) does not promote swelling of Laponite then rendering the attachment of the organomodified alkoxide to the clay external surface resulting in this case in the reduction of the specific surface area, as well as increasing the hydrophobicity of these materials.

The thermogravimetric curves of parent Laponite and of one representative sample, namely, Lap-Biu, are included in Fig. II.6; the curves from the other solids are included in Fig. II.S1; a summary of the mass losses at different temperature intervals for all the samples studied is given in Table II.3. The TG curve for Laponite shows mass losses related to removal of adsorbed water and to dehydroxylation of the layers, amounting 19% of the initial mass of the sample. The first mass loss is associated to an endothermic event centered at 85 °C, while the second mass loss is associated to an endothermic effect at 712ºC, due to the dehydroxylation of the solid and an exothermic event centered at 747°C, due to the subsequent phase change from Laponite to enstatite and silica that occurs immediately after the dehydroxylation.

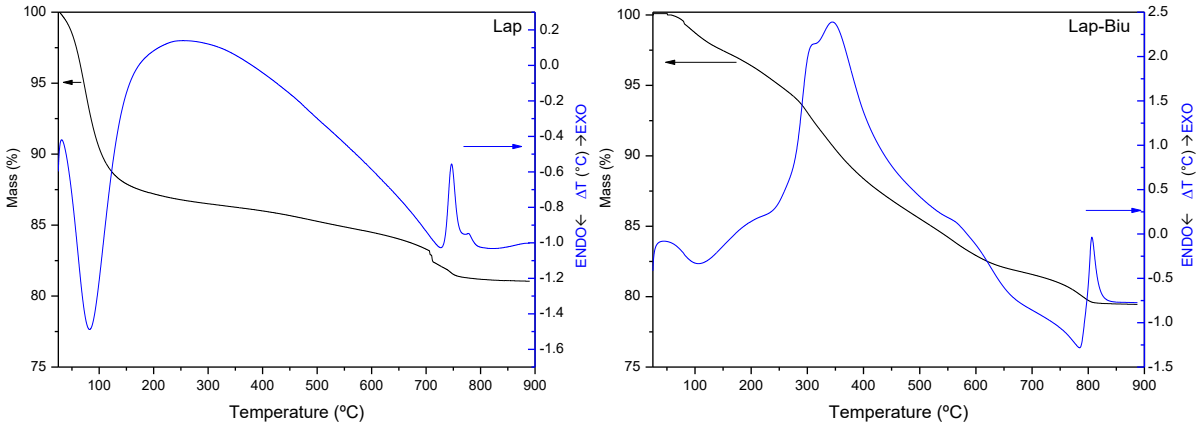

Fig. II.6. Thermogravimetric curves of Lap and Lap-Biu solids.

The curves for all the functionalised samples are composed of an initial mass loss corresponding to the removal of adsorbed water, a central loss of the organic matter, composed of various overlapped effects, and finally the dehydroxylation of Laponite. The first effect is much less intense in the functionalised samples than in parent Laponite, and it accounts only for 1-4% of the initial mass of the solids; the organofunctionalisation process induces hydrophobicity in the solids and strongly decrease the amount of adsorbed water, mainly when the reactions are carried out under non-aqueous conditions and the exchangeable cations are removed. This mass loss is always associated to an endothermic effect, centered between 85 and 106ºC.

The organic matter incorporated in the solids is removed in the temperature range ca. 150 - 650°C. The mass loss is observed in several consecutive, overlapped, steps, without the existence of *plateaux* corresponding to the formation of thermally stable intermediates, in

agreement with the presence of a very broad exothermic effect, also with shoulders corresponding to secondary effects, in the DTA curves. This may be due to the progressive removal of different fragments of the organic molecules, and to the existence of molecules in different environments, retained with different strengths. The process gives rise to a strong exothermic effect, related to combustion of the organic components of the samples. The masses of the final residues were between 74-80% of the initial masses, in agreement with the compositions given by chemical analyses. No significant differences were observed when using biuret or melamine as aminated molecules, the removal of both molecules took place in a similar way and at similar temperatures; the preparation method did not influence significantly the thermal behavior of the solids.

The last mass loss, corresponding to dehydroxylation of Laponite, was considerably delayed, even 90ºC, in the functionalized materials, in comparison with the temperature at which it is recorded for parent Laponite. Thus, this loss was centered at 791-803ºC in the functionalized solids, and was recorded as a broader process than in the natural Laponite, while the associated endothermic effect is also recorded at higher temperatures in the functionalised solids (783-792ºC). This may be mainly due to the "protection" of the clay layers by the SiO_2 formed by the thermal decomposition of the aminosilane incorporated, which may also hinder transmission of heat to the clay layers, and removal of the water generated. Accordingly, the final phase change to form enstatite is also delayed, the associated exothermic effect being centered at 807-809ºC (747ºC for natural Laponite), the higher amount of SiO_2 now available to form the high temperature phase may delay the final phase transformation.

Table II.3

Mass losses (%) in different temperature ranges.

	T_i-150°C	150-650°C	650-T_f	Total
Lap	12.1	3.9	3.0	19.0
Lap-Biu	2.5	15.4	2.6	20.5
Lap-BiuH	3.8	19.7	2.1	25.6
Lap-Mel	2.3	18.0	2.9	23.2
Lap-MelH	3.9	15.1	3.0	22.0

T_i and T_f: Initial and final temperature, respectively

From SEM analysis (Fig. II.7), it is observed that the functionalised solids have a much spongier morphology than parent Laponite (Borsacchi et al., 2007), and among them, the materials obtained by the aqueous route are less spongy than those obtained by the non-hydrolytic route, which showed the spongiest morphology. This confirms that the synthetic route followed influenced the surface structure of the obtained materials.

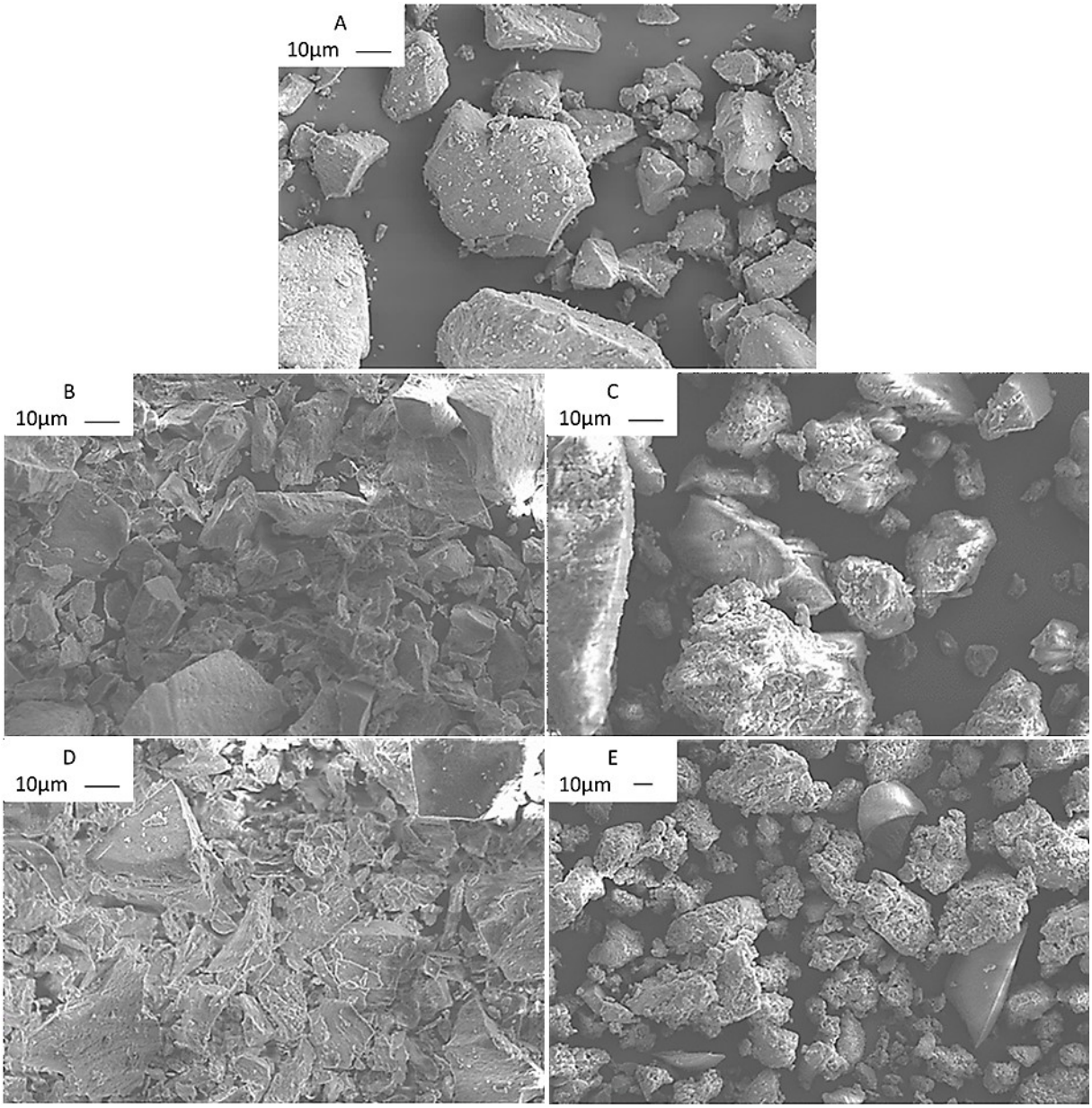

Fig. II.7. SEM micrographs of the solids Lap (A), Lap-Biu (B), Lap-BiuH (C), Lap-Mel (D) and Lap-MelH (E).

3.2. Adsorption study

3.2.a. Kinetics study. Adsorption of TMP (Fig. II.8) was a very fast process and the equilibrium was attained within 20 minutes. Mathematical models (Xi et al., 2010) were applied to the experimental results to determine what of them best described the process. The pseudo-first-order model provided a better fit to the experimental data, and the compounds prepared by the aqueous route showed higher affinity for TMP, with higher rate constants, than the materials obtained by the non-aqueous route. Results reported in the literature for adsorption of TMP on other clay materials (Bekçi et al., 2007; Molu and Yurdakoç, 2010) indicate that the process is best described by the pseudo-second-order mathematical model, where the adsorption rate is controlled by the chemical interaction between the components of the liquid/solid interface, but in Laponite-based materials the pseudo-first-order model shows a better fit (De Carvalho et al., 2010; Qiu et al., 2009).

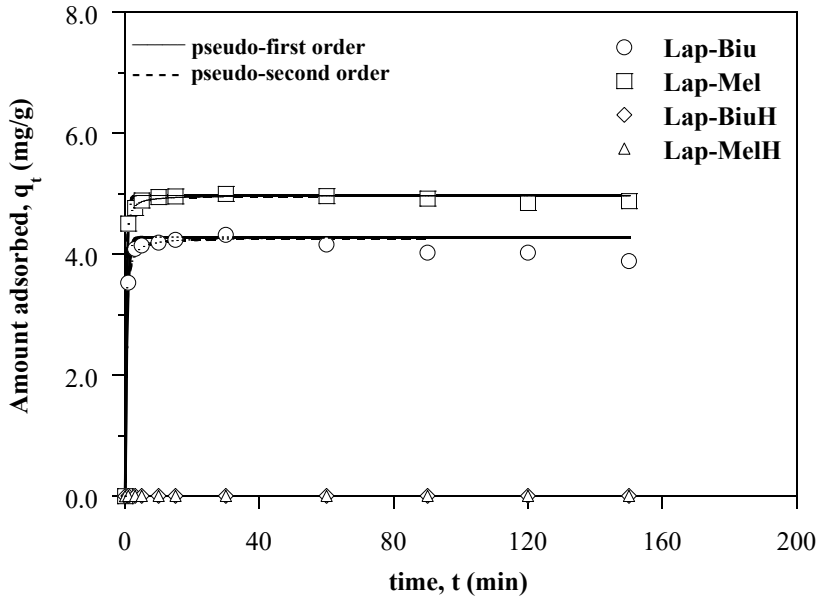

Fig. II.8. Kinetics study of TMP adsorption on Lap-Biu, Lap-BiuH, Lap-Mel and Lap-MelH, and application of the mathematical models of pseudo-first order, pseudo-second order. Symbols: experimental values; lines; fitted model.

To know the adsorption kinetics is a fundamental point in adsorption studies, giving valuable evidences of the possibility of technological application of an adsorbent for a particular separation process. The pseudo-first-order and the second-order kinetic models

were used to elucidate the adsorption mechanism. The pseudo-first-order kinetics model is described by Equation 3 (Lagergren, 1898):

$$q_t = q_e \cdot \left[1 - \exp\left(-k_1 \cdot t\right)\right] \qquad \text{Equation 3}$$

where q_e and q_t (mg/g) are the amounts of adsorbate adsorbed at equilibrium and at time t, respectively, and k_1 is the rate constant (min^{-1}).

The pseudo-second-order kinetic model is described by Equation 4 (Ho and Ofomaja, 2006):

$$q_t = \frac{k_2 \cdot q_e^2 \cdot t}{1 + k_2 \cdot q_e \cdot t} \qquad \text{Equation 4}$$

where q_e is the maximum adsorption capacity (mg/g), q_t is the amount of adsorbate (mg/g) adsorbed at time t (min) and k_2 is the rate constant (g/(mg·min)).

The intra-particle diffusion model, based on the theory by Weber and Morris (Weber and Morris, 1963), was used to identify the applicability of the diffusion mechanism. According to this theory, the adsorbate uptake q_t changes linearly with the square root of the contact time (Equation 5):

$$q_t = k_d \, t^{1/2} + C \qquad \text{Equation 5}$$

where k_d (mg/g·$min^{1/2}$) is a measure of the diffusion coefficient and C is an intraparticle diffusion constant (mg/g) directly proportional to the boundary layer thickness.

The nonlinear chi-square test (χ^2) is a statistical tool necessary to describe the best fit in an adsorption system; it is determined from the sum of the square differences between the experimental and calculated data, with each squared difference divided by its corresponding value (calculated from the theoretical adsorption models), Equation 6. Thus, small X^2 values indicate a good fitting, while a larger value represents deviation of the experimental data.

$$X^2 = \sum_{i=1}^{n} \frac{\left(q_{t_{calc}} - q_{t_{exp}}\right)^2}{q_{t_{exp}}} \qquad \text{Equation 6}$$

The kinetic parameters for the adsorption of TMP on the hybrid materials were calculated from the corresponding plots and are included in Table II.4. The best fit was achieved with the pseudo-first-order kinetic model, evidencing that the adsorption process occurred by a physisorption mechanism.

The acid catalysis in the aqueous route compared to the non-hydrolytic route alters the amount of TMP adsorbed on the clay surface and consequently influences the amount of amine groups attached to the clay. Broadly speaking, the samples prepared by the non-hydrolytic procedure promote removal of TMP until the equilibrium is reached. This fact could be due to the presence of organic units on the clay surfaces and also to the presence of larger amounts of amine groups from melamine or biuret molecules bound to ClPTES. Thus, both the time required to reach the equilibrium and the adsorption capacity could be drastically influenced by the synthetic route followed for organofunctionalization. So, for samples Lap-Biu and Lap-BiuH the kinetics study shows that organofunctionalization modifies the adsorption capacity (q_t = 4.32 mg/g and 0.0043 mg/g, respectively), while for samples Lap-Mel and Lap-MelH the values were q_t = 4.87 mg/g and 0.0050 mg/g, respectively.

Table II.4

Pseudo-first order, pseudo-second order and intraparticle diffusion kinetic parameters for TMP adsorption.

	Lap-Biu	Lap-Mel
Pseudo-first order		
k_1 (min^{-1})	1.72	2.36
q_e (mg/g)	4.28	4.97
χ^2	0.36	0.076
R^2	0.97	0.996
Pseudo-second order		
k_2 (g/(mg·min))	1.15	1.93
q_e (mg/g)	4.28	4.97
χ^2	0.30	0.030
R^2	0.98	0.998
Intraparticle diffusion		
k_d ($mg/(g \cdot min^{1/2})$)	0.068	0.080
C (mg/g)	3.98	4.67
R^2	0.98	0.790

The adsorption capacity q_e at equilibrium calculated for the pseudo-first order kinetics fits very well with the experimental value. This suggests that the pseudo-first order is the predominant mechanism and that the overall rate of TMP adsorption is controlled by the formation of hydrogen bonds between the amine groups in the hybrid materials and TMP, as it has been confirmed by an FTIR study. Fig. II.9 and Fig. II.S2 show the spectra of laponite-functionalized derivatives before and after adsorption of TMP. After adsorption, bands centred around 3358 and 1633 cm^{-1} are observed, in all the cases broader than before adsorption and assigned to the OH stretching and bending modes, respectively, of water molecules. The presence of bands due to hydrogen bonds between TMP and NH_2 groups from solids, which should be recorded in the first region, cannot be definitively confirmed or discarded. The main change induced by the presence of TMP is the shifting and strong enhancement of the hydroxyl band, evidencing the interaction via hydrogen bonding with OH from the clay matrix. The presence of TMP on the surface of the solids was also confirmed by the presence of the bands at 2952 and 2892 cm^{-1}, assigned to C-H stretching modes of aliphatic groups.

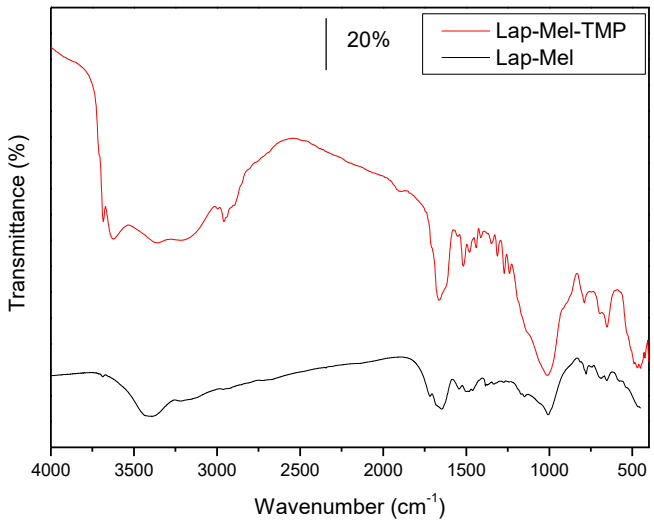

Fig. II.9. FTIR spectra demonstrating the interaction between Lap-Mel and TMP.

The *fractional attainment at equilibrium* is the ratio between the amount of adsorbate removed from solution after a given time (q_t) and that removed when the adsorption equilibrium (q_e) is attained, Eqn. 7.

$$\alpha_e = q_t/q_e \qquad \text{Equation 7}$$

It would be definitely expected that factors such as the number of active adsorption sites on the adsorbate surface and the bulkiness of the adsorbate molecule would affect the rate of adsorption of TMP. However, further more information can be obtained from the fractional attainment at equilibrium. The rate of the attainment of equilibrium may be either film-diffusion controlled or particle-diffusion controlled, even though these two mechanisms cannot be sharply demarcated (Okeimen et al., 1999).

The plot of α_e against time for Lap-Biu and Lap-Mel is shown in Fig. II.10. The adsorbents showed high adsorption capacities in the first stages of the adsorption process, until 5 minutes. The value of α_e for sample Lap-Biu sharply increases in the early steps of the process and converges to one at 15 min. However, for sample Lap-Mel it converges to one even within one minute, confirming the fast removal of TMP from solution. The higher removal rate could be related to the presence of amine groups well dispersed on the clay surface, as evidenced by the lower specific surface area measured for this solid.

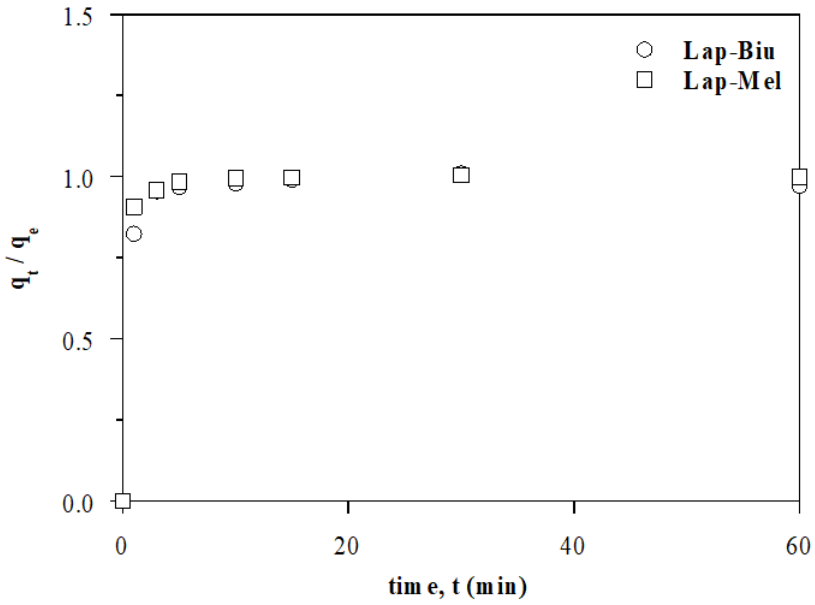

Fig. II.10. Fractional attainment at equilibrium (α_e) against time for TMP uptake by Laponite hybrid materials.

As previously observed with fibrous clays and saponites (Marçal et al., 2015), the presence of organic molecules on the surface may promote a negative effect on the final adsorption capacity. However, the current results suggest that the organic chains from biuret and melamine and the alkoxide groups are well dispersed on the clay platelets in the samples prepared by the non-hydrolytic route and could favor the adsorption of TMP. On the contrary,

the aqueous synthesis in acidic conditions promotes the agglomeration of organic molecules and the possible active sites (amine groups from biuret and melamine) are not available for adsorption of further molecules onto the surface due to their binding to the surface (Fig. II.8). This result agrees well with the previously reported studies on saponite and fibrous clays grafted with amine groups (Marçal et al., 2015; Moreira et al., 2016), where the presence of well-dispersed active sites favors the adsorption process; however if they are in excess, these sites could hinder the adsorption of the target compounds.

3.2.b. Equilibrium study. The data on adsorption at equilibrium of TMP on the organically modified Laponite were fitted by applying the Langmuir, Freundlich, and Sips isotherm models.

The *Langmuir* adsorption model predicts that a monolayer of adsorbate molecules covers the outer surface of the adsorbent; adsorption takes place at specific homogeneous sites of the adsorbent surface, which implies that all adsorption sites are identical and energetically equivalent (Langmuir, 1916). The Langmuir adsorption isotherm has been successfully applied to many adsorption processes involving organic compounds. It equation describing the process can be written as:

$$q_e = \frac{q_L \cdot k_L \cdot C_e}{1 + k_L \cdot C_e} \qquad \text{Equation 8}$$

where both q_L (mg/g) and k_L (dm^3/mg) are Langmuir constants related to the monolayer adsorption capacity.

The *Freundlich* equation is an empirical equation used to describe adsorption on heterogeneous systems. It is usually written as (Freundlich, 1906):

$$q_e = k_F \cdot C_e^{1/m_F} \qquad \text{Equation 9}$$

where k_F and m_F are empirical constants related to the extent of adsorption and its efficacy, respectively.

The *Sips* isotherm is a combined form of the Langmuir and Freundlich models deduced for predicting the adsorption on heterogeneous systems and circumventing the

limitation of the rising adsorbate concentration associated to the Freundlich isotherm model (Sips, 1948). At low adsorbate concentrations, it is simplified to the Freundlich isotherm, while at high adsorbate concentrations, it predicts a monolayer adsorption capacity characteristic of the Langmuir isotherm. The corresponding equation is:

$$q_e = \frac{q_S \cdot k_S \cdot C_e^{m_S}}{1 + k_S \cdot C_e^{m_S}} \qquad \text{Equation 10}$$

where k_S (dm^3/mg) and q_s (mg/g) are the Sips constants representing the adsorption energy and the monolayer adsorption capacity, respectively, and m_S is an empirical constant.

For evaluating the efficiency of the adsorbents, the equilibrium adsorption was studied as a function of the equilibrium concentration (Fig. II.11, Table II.5) applying all three models above described. According to Giles classification (Giles and Smith, 1974), the isotherms were type L4 for Lap-Mel and L3 for the other adsorbents. L-type or Langmuir isotherms are characterized by a non-linear concave inclination with respect to the abscissa axis, indicating a decreasing availability of adsorption sites when the concentration at equilibrium increases (Bekçi et al., 2006; Marçal et al., 2015). Good fitting results were obtained for all samples. Sample Lap-Mel showed the highest adsorption capacity, with q_e = 65.73 mg/g, while the values for samples Lap-Biu, Lap-BiuH and Lap-MelH were q_e = 43.12, 38.73 and 30.75 mg/g, respectively. The regression coefficients were higher than 0.93, and the Sips model (Sips, 1948) showed the best fitting among all models considered.

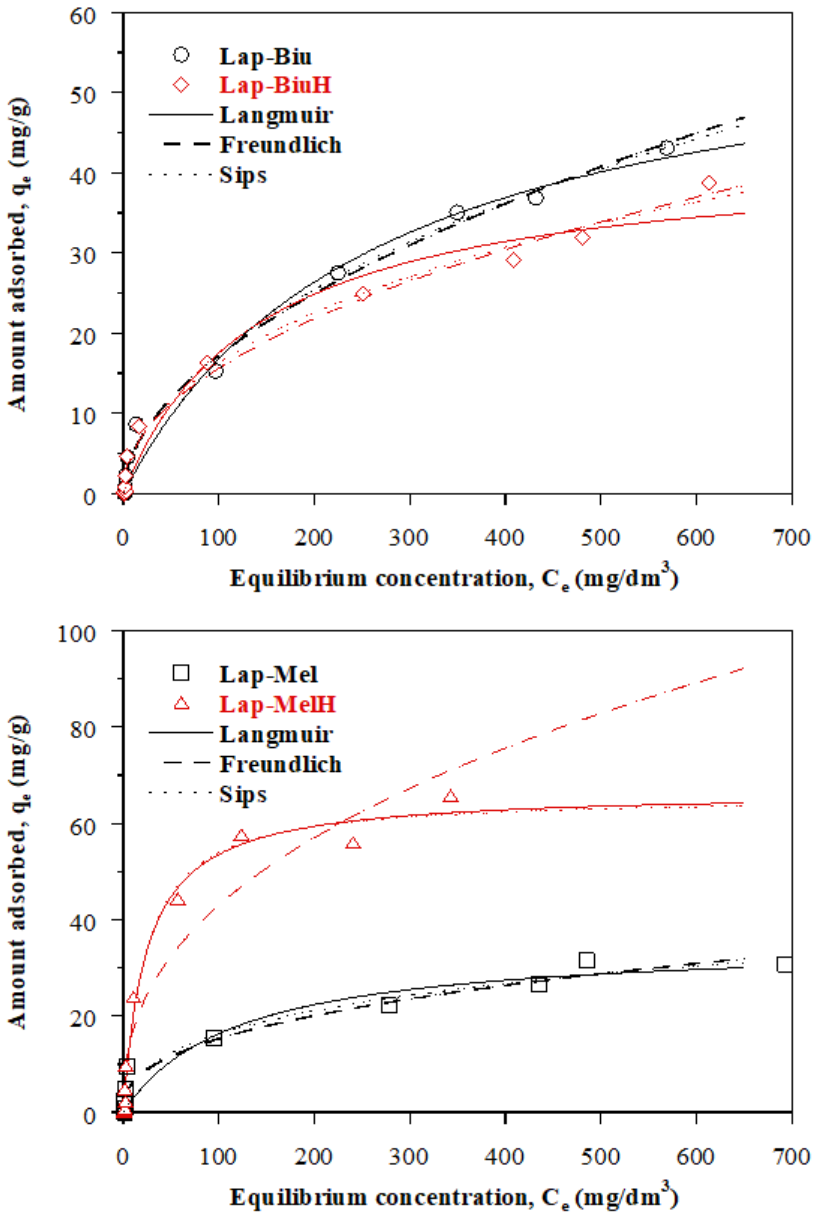

Fig. II.9. Equilibrium study of TMP on Lap-Biu, Lap-BiuH, Lap-Mel and Lap-MelH, and application of the mathematical models of Langmuir, Freundlich and Sips.

Table II.5

Langmuir, Freundlich and Sips equation parameters for the TMP adsorption by modified Laponites.

Adsorbent	Lap-Biu	Lap-BiuH	Lap-Mel	Lap-MelH
Langmuir				
q_L (mg/g)	61	43	35	67
k_L (dm^3/mg)	0.0038	0.0070	0.0086	0.0041
χ^2	53	62	111	102
R^2	0.98	0.970	0.930	0.985
Freundlich				
k_F (mg/g)	1.46	1.71	2.51	6.59
m_F	1.87	2.1	2.5	2.4
χ^2	27	30	67	532
R^2	0.991	0.98	0.96	0.930
Sips				
q_s (mg/g)	226	141	83	66
k_S (dm^3/mg)	0.0055	0.010	0.027	0.038
m_S	0.59	0.55	0.48	1.04
χ^2	26	28	63	101
R^2	0.991	0.98	0.96	0.980

Melamine-derived materials showed the highest percentages of TMP removal, rapidly reaching 99%, which was maintained constant for a long time in the case of the sample prepared by the non-hydrolytic method and slowly decreased for that prepared by the hydrolytic method. After the equilibrium was reached, the desorption process begins (in some cases), a fact that can be attributed to the saturation of the active sites of the solid materials, reducing the efficiency of the process at times larger than the ideal time observed in the kinetic study.

A comparison of the results with those from other adsorbents reported in the literature is given in Table II.6, showing the good performance of the adsorbents studied in this report.

Table II.6

Comparison of the TMP maximum adsorption capacity of the adsorbents prepared in this work with other adsorbents employed in the literature.

Adsorbent	Maximum adsorption capacity (mg/g)	Reference
Lap-Biu	43.12	This work
Lap-BiuH	38.73	This work
Lap-Mel	30.75	This work
Lap-MelH	65.73	This work
Montmorillonite	26.28-46.45	(Molu and Yurdakoç, 2010)
Sewage sludge and fish waste	3.63-6.53 (650 °C) 9.00-13.94 (950 °C)	(Nielsen and Bandosz, 2016)
Activated Carbon activated by phosphorus oxyacids	58.06-78.39	(Liu et al., 2012)

4. Conclusions

New nanohybrid materials based on functionalized derivatives of Laponite were prepared by two routes: organic solvent and aqueous medium under acidic catalysis. The acidic catalysis on hydrolitic method promotes the hydrolysis of the alkoxide, resulting in materials with high specific surface areas. Specifically, Lap-MelH exhibits a larger specific surface area than the starting purified Laponite. All the differences in the physico-chemical properties of the hybrids and in the adsorptive properties of the four materials were carefully evaluated.

The textural characteristics and the presence of the surface functional groups (melamine or biuret) on the Laponite hybrid derivatives strongly depend on the nature of the synthesis route followed, toluene non-aqueous or aqueous under acidic conditions.

The probable interactions of trimethoprim with Laponite nanohybrid derivatives occur by hydrogen bonding and Lewis acid–base interactions and cation exchange. In this sense the presence of organic moieties on the surface or interlayer surface on the Laponite functionalized derivatives also plays an important role.

These strategy synthesis open new possibilities to immobilize important and active molecules such as drugs, catalysts and photocatalysts, among others, on the clay mineral surface or interlayer space.

References for Article II

Bandeira, L.C., Calefi, P.S., Ciuffi, K.J., de Faria, E.H., Nassar, E.J., Vicente, M.A., Trujillano, R., 2012. Preparation of composites of laponite with alginate and alginic acid polysaccharides. Polym. Int. 61, 1170–1176. https://doi.org/10.1002/pi.4196

Bekçi, Z., Seki, Y., Kadir Yurdakoç, M., 2007. A study of equilibrium and FTIR, SEM/EDS analysis of trimethoprim adsorption onto K10. J. Mol. Struct. 827, 67–74. https://doi.org/10.1016/j.molstruc.2006.04.054

Bekçi, Z., Seki, Y., Yurdakoç, M.K., 2006. Equilibrium studies for trimethoprim adsorption on montmorillonite KSF. J. Hazard. Mater. 133, 233–242. https://doi.org/10.1016/j.jhazmat.2005.10.029

Ben Zid, T., Fadhli, M., Khedher, I., Fraile, J.M., 2017. New bis (oxazoline)–vanadyl complexes, supported by electrostatic interaction in Laponite clay, as heterogeneous catalysts for asymmetric oxidation of methyl phenyl sulfide. Micropor. Mesopor. Mater. 239, 167–172. https://doi.org/10.1016/j.micromeso.2016.09.055

Borsacchi, S., Geppi, M., Ricci, L., Ruggeri, G., Veracini, C.A., 2007. Interactions at the surface of organophilic-modified laponites: A multinuclear solid-state NMR study. Langmuir 23, 3953–3960. https://doi.org/10.1021/la063040a

Christidis, G.E., 2013. Chapter 4.1 – Assessment of Industrial Clays, 2nd ed, Developments in Clay Science. Elsevier Ltd. https://doi.org/10.1016/B978-0-08-098259-5.00017-2

De Carvalho, T.E.M., Fungaro, D.A., De Izidoro, J.C., 2010. Adsorção do corante reativo laranja 16 de solução es aquosas por zeólita sintética. Quim. Nova 33, 358–363. https://doi.org/10.1590/S0100-40422010000200023

de Paiva, L.B., Morales, A.R., Valenzuela Díaz, F.R., 2008. Organoclays: Properties, preparation and applications. Appl. Clay Sci. 42, 8–24. https://doi.org/10.1016/j.clay.2008.02.006

Detellier, C., Letaief, S., 2013. Kaolinite-polymer nanocomposites, 2nd ed, Developments in Clay Science. Elsevier Ltd. https://doi.org/10.1016/B978-0-08-098258-8.00022-5

Freundlich, H.M.F., 1906. Over the Adsorption in Solution. Z. Phys. Chem. 57, 385–471.

Giles, C.H., Smith, D., Huitson, A., 1974. A General Treatment and Classification of the Solute Adsorption Isotherm. I. Theoretical. J. Colloid Interf. Sci., 47, 755–765. https://doi.org/10.1016/0021-9797(74)90252-5

Ho, Y.S., Ofomaja, A.E., 2006. Biosorption thermodynamics of cadmium on coconut copra meal as biosorbent. Biochem. Eng. J. 30, 117–123. https://doi.org/10.1016/j.bej.2006.02.012

Hua-Feng, P., 2017. Biuret-assisted formation of nanostructured In_2O_3 architectures and their photoluminescence properties. J. Lumin. 182, 8–14. https://doi.org/10.1016/j.jlumin.2016.10.014

Iurascu, B., Siminiceanu, I., Vione, D., Vicente, M.A., Gil, A., 2009. Phenol degradation in water through a heterogeneous photo-Fenton process catalyzed by Fe-treated laponite. Water Res. 43,

1313–1322. https://doi.org/10.1016/j.watres.2008.12.032

Ji, Y., Xie, W., Fan, Y., Shi, Y., Kong, D., Lu, J., 2016. Degradation of trimethoprim by thermo-activated persulfate oxidation: Reaction kinetics and transformation mechanisms. Chem. Eng. J. 286, 16–24. https://doi.org/10.1016/j.cej.2015.10.050

Lagaly, G., Dékány, I., 2013. Colloid clay science, http://dx.doi.org/10.1016/B978-0-08-098258-8.00010-9; Chapter 8 (pp. 243–345) in: Handbook of Clay Science, 2nd Edition (Bergaya, F., Lagaly, G., Eds.). Elsevier. ISBN 9780080993645

Lagaly, G., Ogawa, M., Dékány, I., 2013. Clay mineral-organic interactions, http://dx.doi.org/10.1016/B978-0-08-098258-8.00015-8; Chapter 10.3 (pp. 435–505) in: Handbook of Clay Science, 2nd Edition (Bergaya, F., Lagaly, G., Eds.). Elsevier. ISBN 9780080993645.

Lagergren, S., 1898. About the theory of so–called adsorption of soluble substances. K. Sven. Vetenskapsakademiens Handl. 24, 1–39.

Langmuir, I., 1916. the Constitution and Fundamental Properties of Solids and Liquids. Part I. Solids. J. Am. Chem. Soc. 252, 2221–2295. https://doi.org/10.1021/ja02268a002

Liu, H., Zhang, J., Bao, N., Cheng, C., Ren, L., Zhang, C., 2012. Textural properties and surface chemistry of lotus stalk-derived activated carbons prepared using different phosphorus oxyacids: Adsorption of trimethoprim. J. Hazard. Mater. 235–236, 367–375. https://doi.org/10.1016/j.jhazmat.2012.08.015

Liu, L., Wan, Q., Xu, X., Duan, S., Yang, C., 2017. Combination of micelle collapse and field-amplified sample stacking in capillary electrophoresis for determination of trimethoprim and sulfamethoxazole in animal-originated foodstuffs. Food Chem. 219, 7–12. https://doi.org/10.1016/j.foodchem.2016.09.118

Marçal, L., de Faria, E.H., Nassar, E.J., Trujillano, R., Martín, N., Vicente, M.A., Rives, V., Gil, A., Korili, S.A., Ciuffi, K.J., 2015. Organically Modified Saponites: SAXS Study of Swelling and Application in Caffeine Removal. ACS Appl. Mater. Interfaces 7, 10853–10862. https://doi.org/10.1021/acsami.5b01894

Molu, Z.B., Yurdakoç, K., 2010. Preparation and characterization of aluminum pillared K10 and KSF for adsorption of trimethoprim. Microporous Mesoporous Mater. 127, 50–60. https://doi.org/10.1016/j.micromeso.2009.06.027

Moreira, M.A., Ciuffi, K.J., Rives, V., Vicente, M.A., Trujillano, R., Gil, A., Korili, S.A., de Faria, E.H., 2016. Effect of chemical modification of palygorskite and sepiolite by 3-aminopropyltriethoxisilane on adsorption of cationic and anionic dyes. Appl. Clay Sci. 135, 394–404. https://doi.org/10.1016/j.clay.2016.10.022

Nielsen, L., Bandosz, T.J., 2016. Analysis of sulfamethoxazole and trimethoprim adsorption on sewage sludge and fish waste derived adsorbents. Microporous Mesoporous Mater. 220, 58–72.

https://doi.org/10.1016/j.micromeso.2015.08.025

Okeimen, F.E., Esther, U.O., David, E.O., 1999. Sorption of Cadmium and Lead ions on modified groundnut husk. Nigerian-Chem. Tech. Biotechnology 31, 97–99.

Pálková, H., Madejová, J., Zimowska, M., Bielańska, E., Olejniczak, Z., Lityńska-Dobrzyńska, L., Serwicka, E.M., 2010. Laponite-derived porous clay heterostructures: I. Synthesis and physicochemical characterization. Microporous Mesoporous Mater. 127, 228–236. https://doi.org/10.1016/j.micromeso.2009.07.019

Pereira, C., Silva, A.R., Carvalho, A.P., Pires, J., Freire, C., 2008. Vanadyl acetylacetonate anchored onto amine-functionalised clays and catalytic activity in the epoxidation of geraniol. J. Mol. Catal. A Chem. 283, 5–14. https://doi.org/10.1016/j.molcata.2007.11.034

Qiu, H., Lv, L., Pan, B., Zhang, Q.Q., Zhang, W., Zhang, Q.Q., 2009. Critical review in adsorption kinetic models. J. Zhejiang Univ. Sci. A 10, 716–724. https://doi.org/10.1631/jzus.A0820524

Richardson, B.J., Lam, P.K.S., Martin, M., 2005. Emerging chemicals of concern: Pharmaceuticals and personal care products (PPCPs) in Asia, with particular reference to Southern China. Mar. Pollut. Bull. 50, 913–920. https://doi.org/10.1016/j.marpolbul.2005.06.034

Sips, R., 1948. On the Structure of a Catalyst Surface. J. Chem. Phys. 16, 490. https://doi.org/10.1063/1.1746922

Stolz, A., Le Floch, S., Reinert, L., Ramos, S.M.M., Tuaillon-Combes, J., Soneda, Y., Chaudet, P., Baillis, D., Blanchard, N., Duclaux, L., San-Miguel, A., 2016. Melamine-derived carbon sponges for oil-water separation. Carbon 107, 198–208. https://doi.org/10.1016/j.carbon.2016.05.059

Weber, W.J., Morris, J.C., 1963. Kinetics of adsorption on carbon from solutions. J. Sanit. Eng. Div. 89, 31–60.

Xi, Y., Mallavarapu, M., Naidu, R., 2010. Preparation, characterization of surfactants modified clay minerals and nitrate adsorption. Appl. Clay Sci. 48, 92–96. https://doi.org/10.1016/j.clay.2009.11.047

Zhang, Y., Wang, A., Tian, X., Wen, Z., Lv, H., Li, D., Li, J., 2016. Efficient mineralization of the antibiotic trimethoprim by solar assisted photoelectro-Fenton process driven by a photovoltaic cell. J. Hazard. Mater. 318, 319–328. https://doi.org/10.1016/j.jhazmat.2016.07.021

Zimowska, M., Gurgul, J., Pálková, H., Olejniczak, Z., Łatka, K., Lityńska-Dobrzyńska, L., Matachowski, L., 2016. Structural rearrangements in Fe-porous clay heterostructures composites derived from Laponite®- Influence of preparation methods and Fe source. Micropor. Mesopor. Mater. 231, 66–81. https://doi.org/10.1016/j.micromeso.2016.05.013

Zimowska, M., Pálková, H., Madejová, J., Dula, R., Pamin, K., Olejniczak, Z., Gil, B., Serwicka, E.M., 2013. Laponite-derived porous clay heterostructures: III. the effect of alumination. Micropor. Mesopor. Mater. 175, 67–75. https://doi.org/10.1016/j.micromeso.2013.02.047

SUPPLEMENTARY MATERIALS FOR ARTICLE II

Table II.S1

Chemical composition (%w/w) of the solids, normalized to water free content, that is the sum of the metallic oxides, C and N being 100% (for the treated solids, the content of elemental C and N was considered, the content of H and O was ignored).

	SiO_2	MgO	Al_2O_3	Fe_2O_3	Na_2O	CaO	C	N	Total
Lap	66.91	29.61	0.06	0.04	3.18	0.21			100
Lap-Biu	71.89	19.73	0.08	0.04	0.16	0.16	7.29	0.7	100
Lap-BiuH	72.86	15.40	0.07	0.04	0.02	0.02	11.20	0.4	100
Lap-Mel	66.53	22.41	0.05	0.04	0.04	0.06	8.68	2.2	100
Lap-MelH	66.72	22.48	0.08	0.04	0.03	0.01	7.21	3.4	100

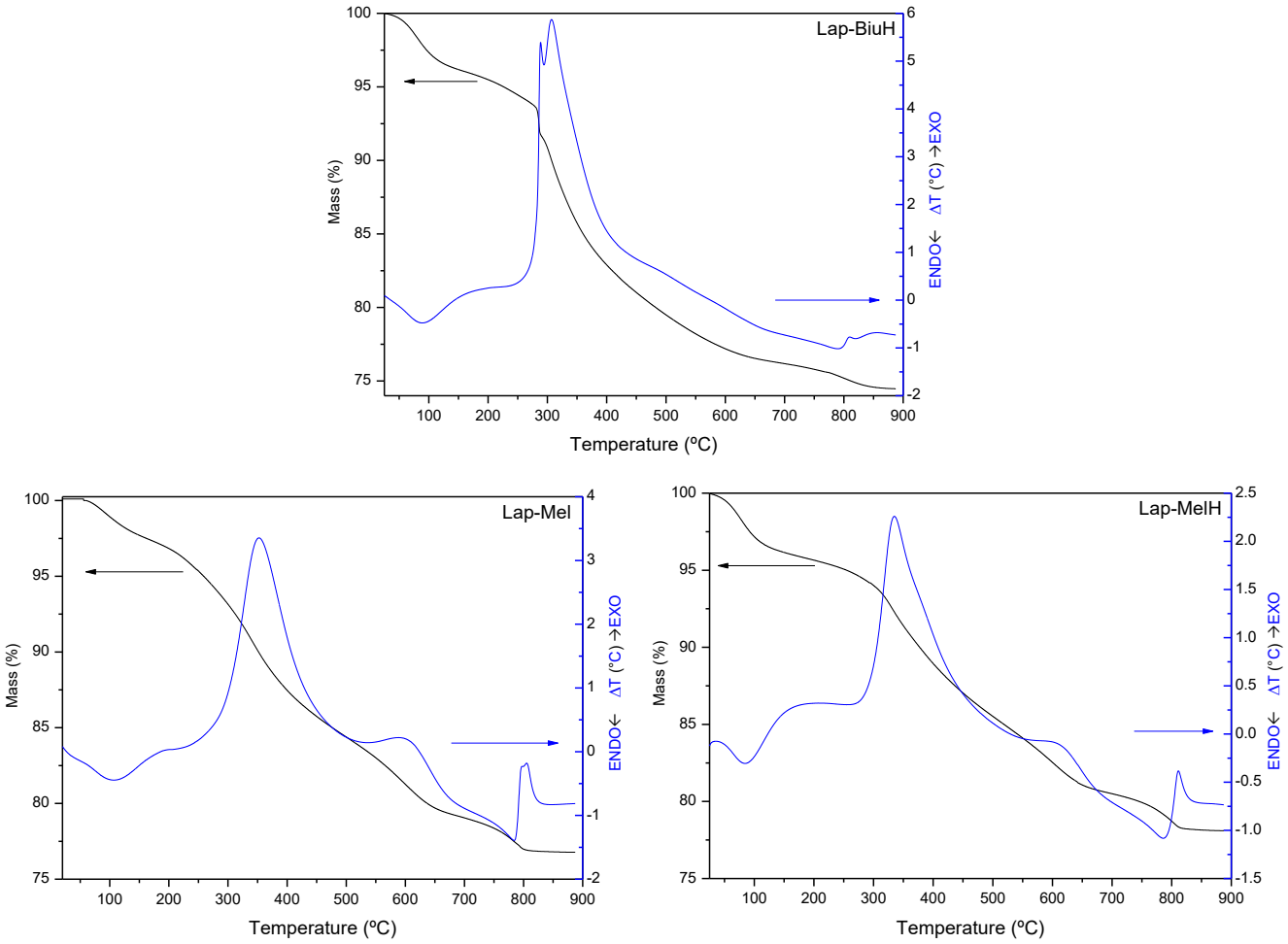

Fig. II.S1. TG and DTA curves of the different materials.

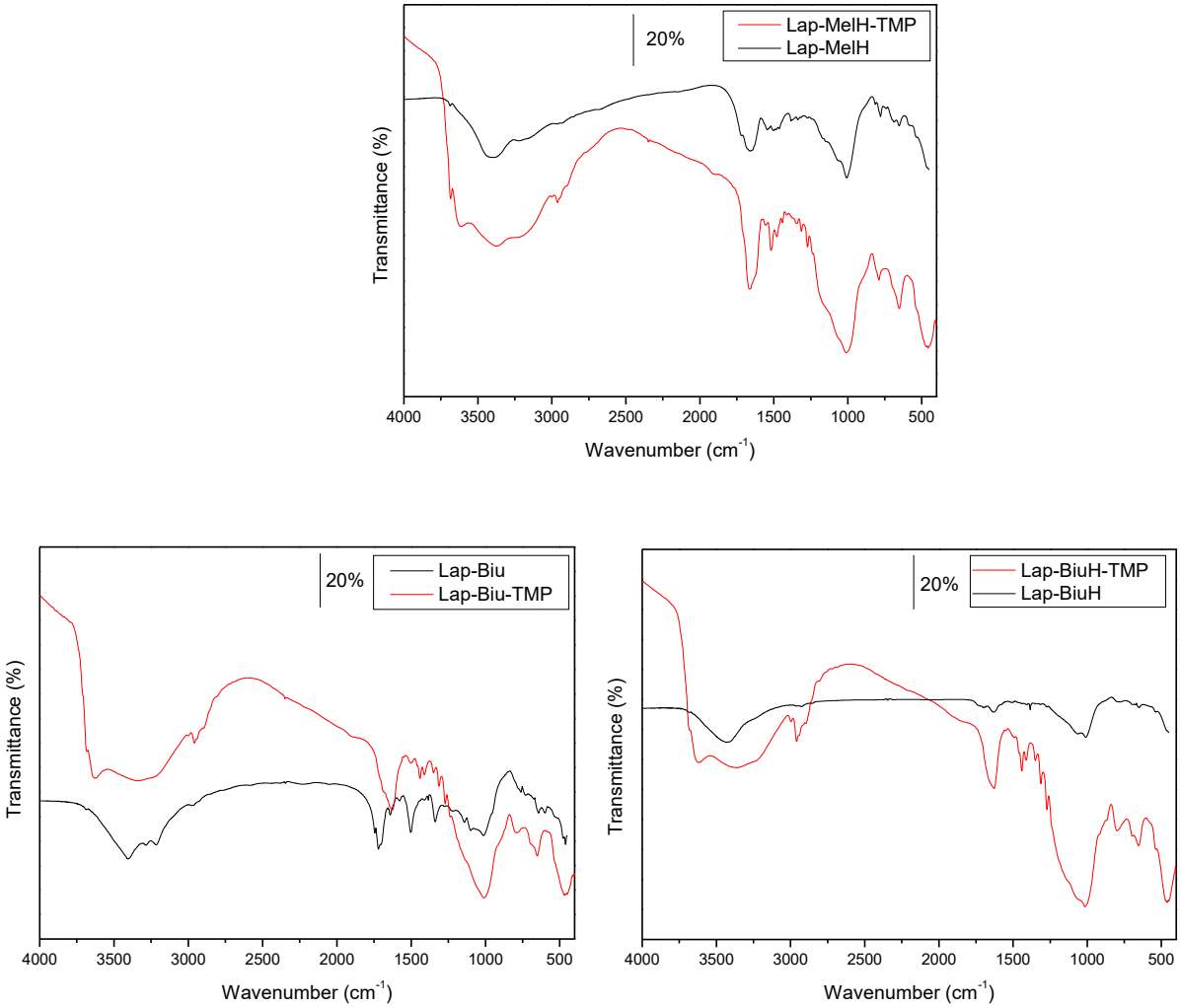

Fig. II.S2. FTIR study of the interaction of Lap-MelH, Lap-Biu and Lap-BiuH solids with TMP.

Scheme I. Probable mechanism involved in laponite functionalization

A. Non-aqueous route

First step: Condensation reaction between the organosilane and each of the amine molecules.

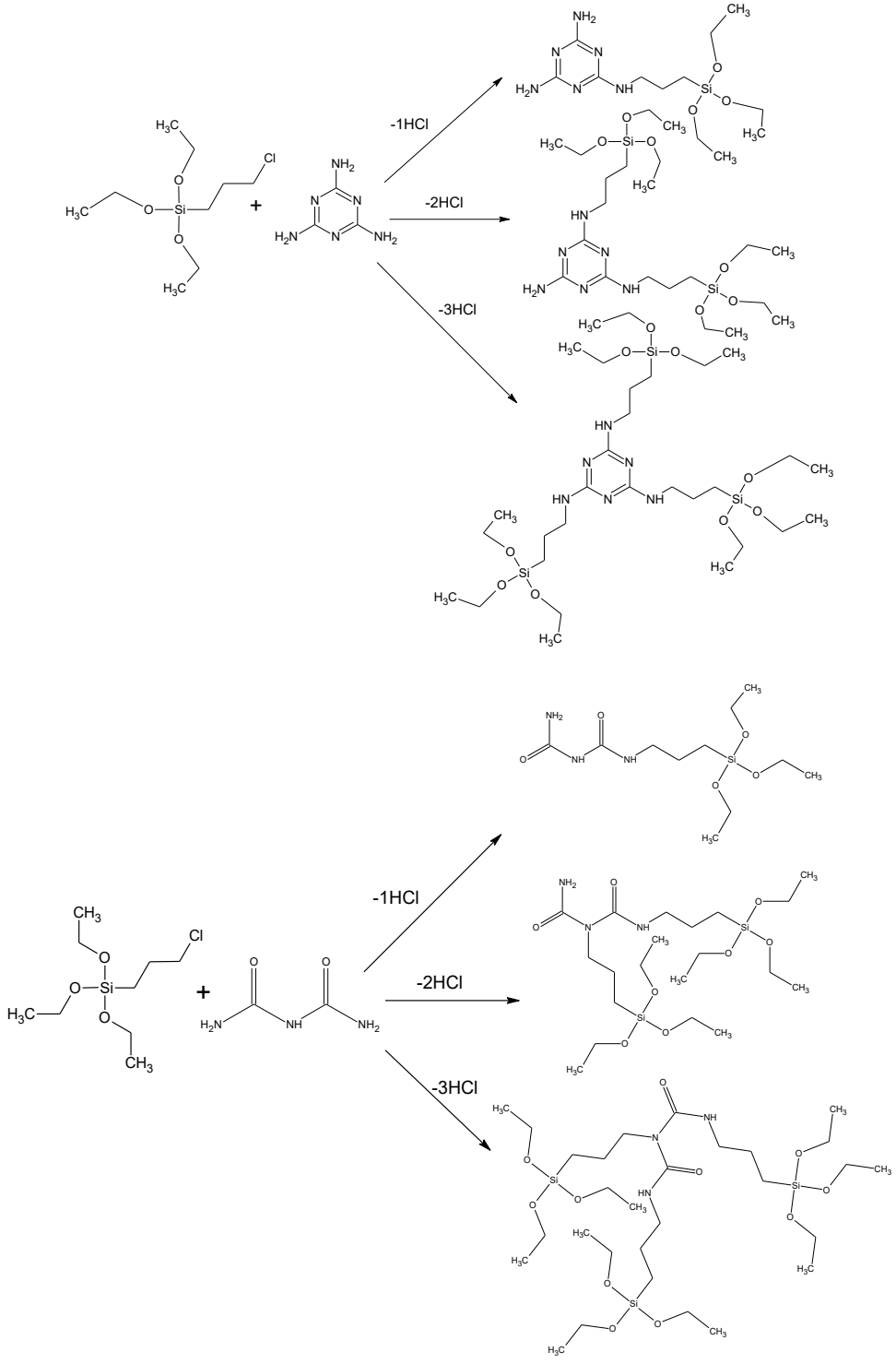

Second step: Condensation with clay silanol groups, hydrolysis and protonation-cation exchange after addition to clay suspension.

B. Aqueous route

First step: Hydrolysis of the alkoxide promoted by water and HCl, and by silanol clay groups.

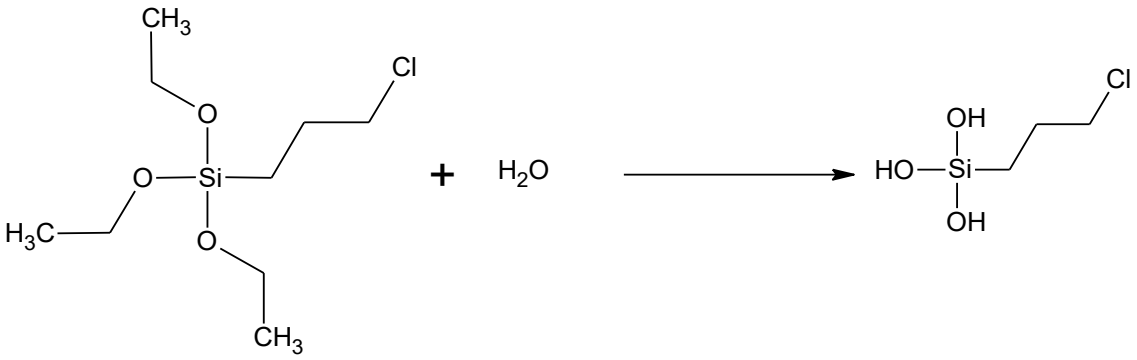

Second step: Condensation of the hydrolyzed alkoxide with the amine molecules.

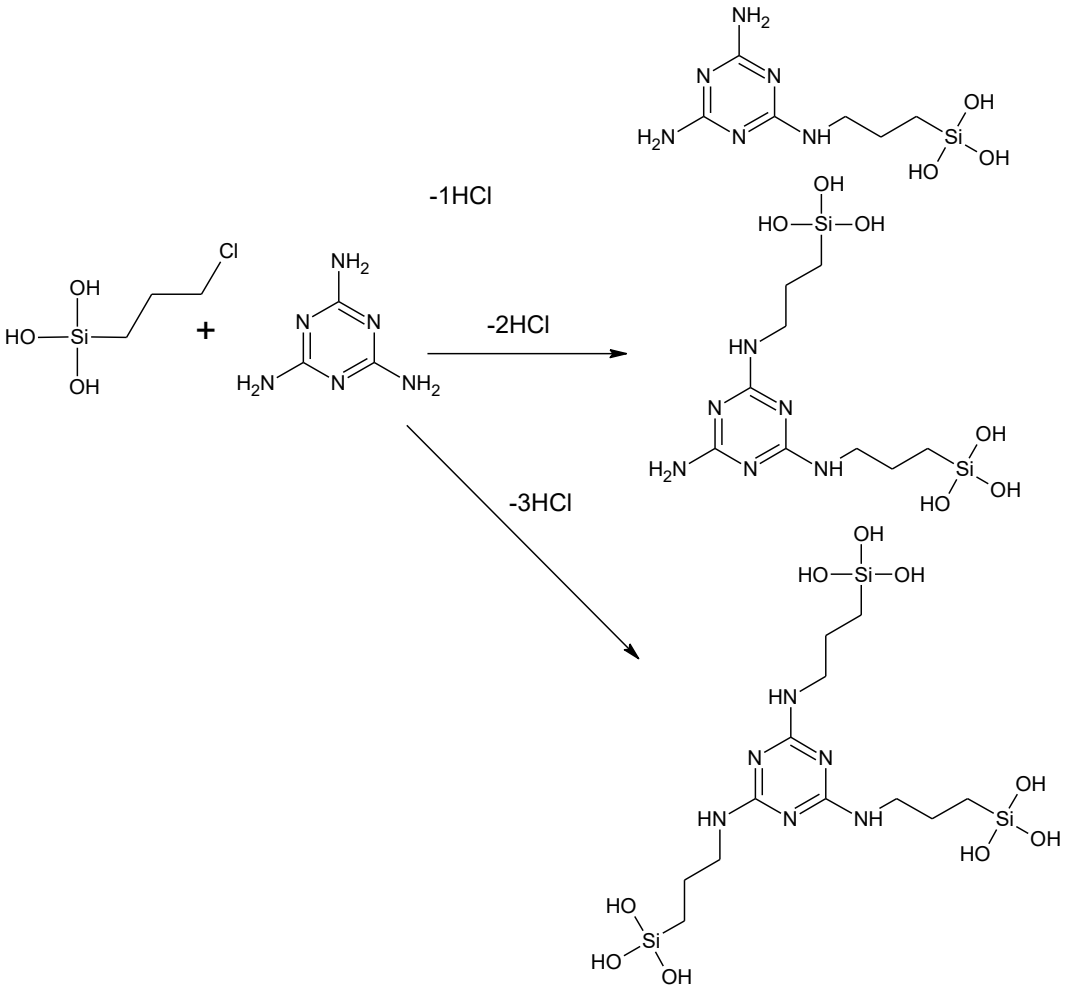

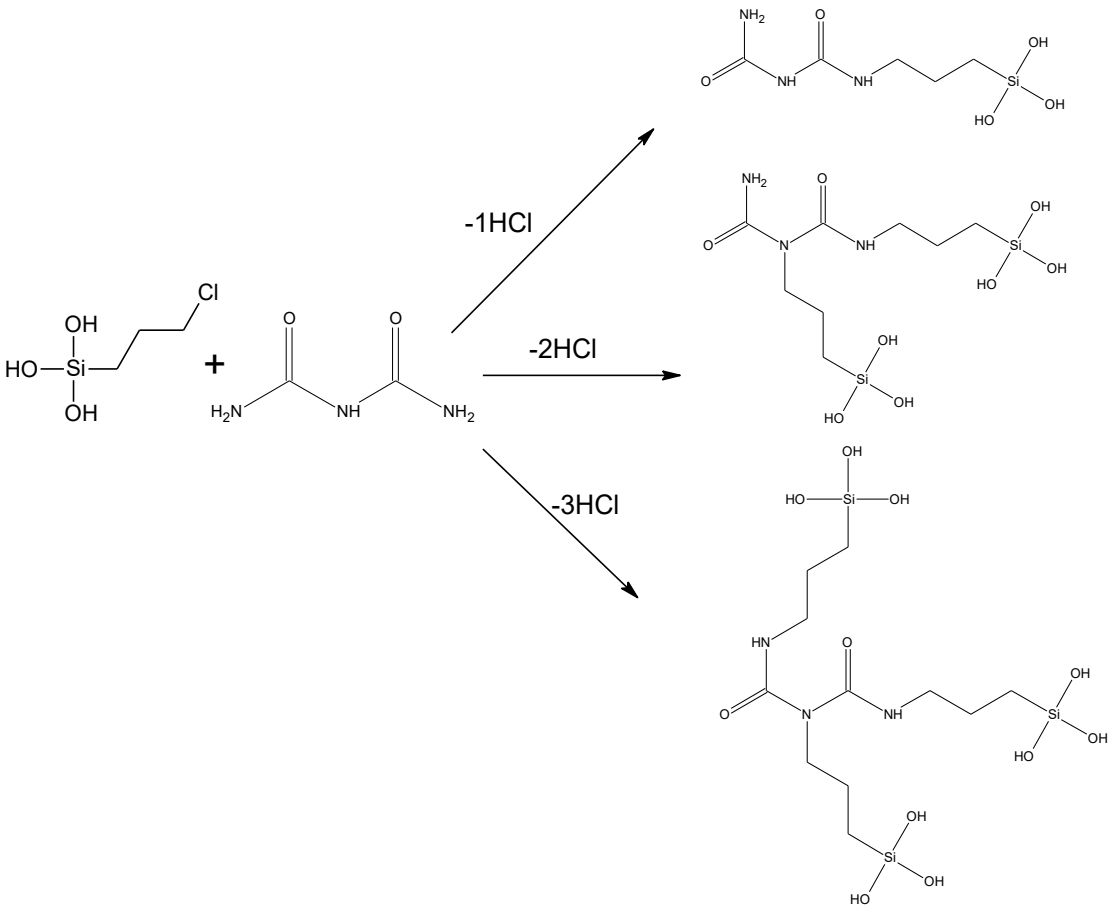

Third step: Condensation with clay silanol groups, and protonation-cation exchange.